Materials Science and Engineering A 527 (2010) 3840–3847

Contents lists available at ScienceDirect

Materials Science and Engineering A

journal homepage: www.elsevier.com/locate/msea

Mechanical and thermal shock behavior of refractory materials for glass feeders

Nicolás Rendtorff[a,b,*], Esteban Aglietti[a,b]

[a] CETMIC (Centro de Tecnología de Recursos Minerales y Cerámica, CIC-CONICET La Plata), Camino Centenario y 506, C.C.49, (B1897ZCA) M.B. Gonnet, Buenos Aires, Argentina
[b] Facultad de Ciencias exactas de la Universidad Nacional de la Plata, Argentina

ARTICLE INFO

Article history:
Received 7 January 2010
Received in revised form 16 February 2010
Accepted 17 February 2010

Keywords:
Refractories
Fracture properties
Thermal shock
Alumina
Mullite
Zircon

ABSTRACT

Refractory materials of the Al_2O_3–SiO_2–ZrO_2 system are widely used in glass industry in forehearth, distributors, feeders, and as expendable materials as they are known to have good thermal shock properties. They are commonly subject to thermal stress during installation. Once installed, the service life is then determined mainly by the corrosion characteristics. In this work three refractories were studied to observe and correlate mechanical properties with thermal shock behavior. The materials and their principal crystalline phases are: AM (Alumina–Mullite 35), Am (Alumina–Mullite 10), and AZ (Alumina–Zircon).

All the materials have similar open porosity and pore size distribution. The mechanical characterization comprises: fracture toughness (K_{IC}), fracture initiation energy (γ_{NBT}) and work of fracture (γ_{WOF}). The dynamic elastic modulus E of the composites was measured by the excitation technique.

The water quenching method was used for the experimental evaluation of the thermal shock resistance (TSR). Thermal cycles with different quenching temperature gradients ΔT were applied and a cyclic water quenching was used for the thermal fatigue resistance (TFR) assessment. The TSR behavior was evaluated by measuring the decrease in E/E_0 ratio where E_0 and E are the dynamic elastic modulus before and after one quenching, respectively. The strength (modulus of rupture, MOR) of materials before and after the TSR test was also measured. The AM material showed the highest E, σ_f (MOR) and K_{IC} values. The elastic modulus remained relatively high (near 80%) up to a ΔT of 500 °C for the three samples. AM showed a higher reduction of E and MOR than Am and AZ. Considering the retained MOR and E with ΔT, Am and AZ have a similar behavior.

Theoretical TS parameters (R, R''' and R_{ST}) were calculated for the refractories. The parameters considering crack initiation (R = theoretical ΔTc) are very similar but their value differs considerably to those ΔTc observed experimentally. This fact can be explained if we consider that the microstructure of refractory materials initially has defects and microcracks. The R''' parameters are the same for all materials. For our materials the R_{ST} parameter reflected the TSR damage.

The best TSR and TFR of AZ followed by Am are due to the microcracks size and their distribution in the microstructure of the materials. In AM refractory the high content and great grain size of Mullite produce the appearance of greater cracks than in the other materials.

The usage of these materials in glass service indicates that the AM material has a low TSR resistance.

1. Introduction

Aluminosilicate based refractories are commonly used in glass processing systems. Other compositions included Zircon to improve corrosion resistance. [1–4] These materials are widely used in the glass industry in forehearth, distributor, feeders, and as expendable materials such as plungers, spouts, tubes, orifice rings. Coarse Alumina and Mullite powders and grains (chamottes) are used in the elaboration of these materials, and during processing and sintering we observe that very little, if any, overall shrinkage occurs. Therefore in order to achieve optimum fired density, and in consequence mechanical strength and resistance to corrosion by molten glass, a very efficient particle packing is required. But currently the open porosity of these materials is of 17–21% with an Alumina–Mullite or Alumina–Zircon matrix.

A material of this kind is prepared by blending controlled proportions of components having particle sizes ranging from multi-millimeter to sub-micrometer. The refractory material can therefore be considered to be developed by the bonding of the finer fractions of particles to each other, and to the surfaces of

* Corresponding author at: CETMIC (Centro de Tecnología de Recursos Minerales y Cerámica, CIC-CONICET La Plata), Camino Centenario y 506, C.C.49, (B1897ZCA) M.B. Gonnet, Buenos Aires, Argentina. Tel.: +54 221 484 0247/0167; fax: +54 221 471 0075.
E-mail addresses: rendtorff@cetmic.unlp.edu.ar, rendtorff@hotmail.com (N. Rendtorff).

0921-5093/$ – see front matter © 2010 Elsevier B.V. All rights reserved.
doi:10.1016/j.msea.2010.02.053

the large grains. These materials are commonly subject to thermal stresses during installation. Once installed, they are known to have good thermal shock properties, so the service life is then determined mainly by its corrosion characteristics when glass contact exists.

The evaluation or testing of the thermal shock resistance (TSR) of refractory materials has been studied by many authors in the passed century, always involving many interacting variable factors and parameters [5,6]. A recent review on refractories TSR testing provides some background regarding the basic material properties and other factors that control TSR of refractory materials [7].

There is not just one simple and universal test to evaluate the TSR of ceramic materials and also capable of extrapolating the actual conditions in service, sample geometry, and thermal cycles. However, some experimental tests consisting in sudden heating and cooling are easily made but they have only a comparative value between similar materials. Testing of TSR can simply be done by visual or microscopic microstructure damage evaluation but this is not a very precise method and it depends strongly on the operator as well as on the experimental conditions.

A practical test to evaluate the thermal shock resistance consists to observe the variation or change of some characteristic properties of the material. The TSR can be evaluated on heating or cooling, but in most methods a sudden cooling step is used owing to its greater severity. A simple method consists in heating the test probe to a desired temperature; followed by rapid cooling to room temperature (referred to us as the quenching method), by immersion in liquids such as water, oil or alcohol [8,9]. A characteristic mechanical property like fracture strength or elastic modulus (E) is measured before and after quenching. In this way the severity of the treatment can be studied by determining the relative drop in mechanical strength (MOR) or elastic modulus after exposure at a given thermal cycle. In addition, the damage in the material can be correlated after application of repeated thermal cycles. This can be done because these properties are related to the microstructure integrity, namely the number, size and shape of cracks developed.

The thermoelastic theory is the first attempt to determine the thermal stresses and to introduce the damage resistance parameters of ceramic material, which is focused in the initiation of the fracture (R and R') [5]. A second approach focuses on crack propagation for more severe conditions of thermal shock than those for crack initiation (R''') [10]. A unified theory of the thermal shock resistance considering the initiation and crack propagation was then proposed [11,12] for high strength refractories with short initial cracks (R'''') and for lower strength refractories with larger initial cracks (R_{ST}) [13]. Both models consider γ_{WOF} and E. Aksel [14] studied the TSR behavior of Alumina–Mullite–Zirconia materials using the quenching technique; he concluded that Zircon appears controlling the mechanical properties and the improvement of the TSR.

In this work three kinds of commercial refractories commonly employed in glass feeders were studied to observe and correlate mechanical properties with thermal shock behavior. A complete mechanical and fracture evaluation of the materials was carried out. The TSR behavior was evaluated by two methods: first by mechanical strength decrease (σ_f; modulus of rupture, MOR) of the materials before and after the TSR was measured, and second by measuring the decrease in the E/E_0 ratio where E_0 and E are the dynamic elastic modulus before and after one quenching, respectively. The results of these two methods were then correlated. Microstructure damage was also observed by SEM. Finally the experimental results were related and compared with the theoretical parameters calculated from the experimental mechanical and fracture properties.

2. Experimental procedures

2.1. Characterization techniques

Probes (25 mm × 25 mm × 150 mm) were cut from long refractory pieces. Density and open porosity of the samples were determined by the water absorption method.

Crystalline phases formed were analyzed by XRD (Philips 3020 equipment with Cu-Kα radiation in Ni filter at 40 kV–20 mA). The dynamic elastic modulus E of the composites was measured by the excitation technique with a GrindoSonic, MK5 "Industrial" Model. Dilatometry of samples was performed using a Netzsch dilatometer up to 1400 °C at a heating rate of 10 °C/min [14,15]. The thermal expansion coefficient α of these materials up to 1000 °C was determined. Microstructural examination was conducted with a scanning electron microscope SEM (Jeol JSM 6360 LV) after polishing the probes surface. The MOR (flexural strength, σ_f) was measured on the bars with rectangular section using the three-point bending test (Universal testing machine INSTRON 4483). A span of 120 mm and a displacement rate of 2.5 mm/min were employed. The fracture toughness (K_{IC}) and the fracture initiation energy (γ_{NBT}) were evaluated by the single edge notched beam method [16,17] using notched bars with notches of 0.3 mm wide and depths between 0.5 and 10 mm. In this method K_{IC} is given by:

$$K_{IC} = \frac{3QLC^{1/2}}{2WD^2}\left[A_0 + A_1\left(\frac{C}{D}\right) + A_2\left(\frac{C}{D}\right)^2 + A_3\left(\frac{C}{D}\right)^3 + A_4\left(\frac{C}{D}\right)^4\right] \quad (1)$$

where Q is the load applied to the notched bar in kg, L is the span, C is the depth of the notch, D is the thickness of the specimen, W is the width of the specimen, and A_0, A_1, A_2, A_3 and A_4 are functions of the ratio (L/D) described in [18]. Eq. (1) can be approximated by the following equation:

$$K_{IC} \cong \sigma_f\sqrt{\pi C} \quad (2)$$

Here σ_f is the flexural strength in MPa. The calculated values of K_{IC}, together with E, were used to estimate the surface energy for the area created by the crack initiation (γ_{NBT}) [17,18] which are related by the following equation.

$$K_{IC} = \sqrt{2\gamma_{NBT}E} \quad (3)$$

where γ_{NBT} can be expressed as

$$\gamma_{NBT} = \frac{{K_{IC}}^2}{2E} = \frac{{\sigma_f}^2\pi C}{2E} \quad (4)$$

The work of fracture γ_{WOF} was measured considering the load (σ)–displacement (ε) curve area (energy) divided by twice the fracture surface area (A) (Eq. (5)) [18].

$$\gamma_{WOF} = \frac{\int \sigma\, d\varepsilon}{2A} \quad (5)$$

In this case the bars (25 mm × 25 mm × 150 mm) were notched with diamond saw (0.3 mm wide) between 8 and 10 mm. deep. The displacement rate applied was 0.1 mm/min. Five bars were notched for the γ_{WOF} evaluation. Finally the critical crack length (Lc) was estimated from Eq. (2)

$$Lc = \left(\frac{K_{IC}}{\sigma_f\sqrt{\pi}}\right)^2 \quad (6)$$

The critical length was also proposed by Hasselman [11] in terms of the surface energy. The values obtained by the two methods differ in a constant:

$$Lc = R'''' = \frac{E\gamma_{WOF}}{{\sigma_f}^2(1-\nu)} \quad (7)$$

The thermoelastic fracture mechanism can be applied when Lc is higher than the maximum length of the defects present in the material. In this case, it can be assumed that larger defects correspond to the coarse grains of the starting materials (≈2–3 mm.).

3. Thermal shock behavior

3.1. Thermal shock test

For the TSR experiments, a water quenching method was used similar to the proposed by the ASTM standard [8]. Thermal cycles with quenching temperature differentials, ΔT of 400, 600, 800, and 1000 °C were applied. The sintered sample was heated at a selected temperature in an electrical furnace in air atmosphere for a period of 90 min and then cooled in a water bath at 25 °C. After quenching, samples were dried at 100 °C and then the damage evaluation was made measuring E by the dynamic excitation technique and the flexural strength (MOR). The TSR damage was also observed using SEM micrographs of the quenched probes contrasted with the micrographs of the original materials.

3.2. Thermal fatigue test

In service, refractory materials are not always submitted to one single thermal shock, but to many of them, the last of which is the one that makes a certain piece fail; in fact the temperature changes may be cyclic. Therefore it is of interest to evaluate the behavior of a certain material after several thermal shock treatments. Thermal fatigue resistance (TFR) evaluation [19–24] consists in the measurement of a certain characteristic property of a material with successive thermal shock treatments. Both the experimental evidence and the theoretical models show certain saturation behavior for the TFR of ceramic materials.

The effect of cracks and microcracks on the elastic modulus was reviewed by Stiffler and Hasselman [25]. Generally the resulting elastic modulus is a function of the number and lengths of the cracks, so the decrease in the elastic modulus after a thermal shock is directly related to the nucleation and propagation of the cracks in the material.

The elastic modulus (E) of a material, if the thermal shock treatment is severe enough, decreases in the first 3–5 cycles and then when the energy provided by the thermal shock is not high enough to propagate the existing cracks, the value of E does not change during the following thermal treatments; this stage is called the saturation stage. A similar behavior is observed with the flexural strength.

3.3. Theoretical thermal shock resistance parameters

The thermoelastic approximation (TEA) proposed by Kingery [5] establishes that the fracture will occur when the thermal stress equals or exceeds material's fracture strength. There R and R' parameters are defined, for $h = \infty$ and h = constant (h = heat transference coefficient), respectively:

$$R = \frac{\sigma_f(1-\nu)}{E\alpha} \tag{8}$$

$$R' = Rk = \frac{k\sigma_f(1-\nu)}{E\alpha} \tag{9}$$

where σ_f is the flexural strength, ν is the Poisson ratio, E is the elastic modulus, α is the thermal expansion coefficient and k is the thermal conductivity. The R (°C) parameter is a theoretical critical thermal difference for the crack initiation ΔTc.

The energy balance approximation (EBA) was developed by Hasselman [11] and establishes that a sample will fracture if the thermoelastic energy is superior to the energy required for the creation of the crack surfaces, assuming that the only energy transferred is the elastic energy from the thermal stresses. The following expressions are deduced for the R''' and R'''' parameters:

$$R''' = \frac{E}{\sigma_f^2(1-\nu)} \tag{10}$$

$$R'''' = R'''\gamma_{WOF} = \frac{E\gamma_{WOF}}{\sigma_f^2(1-\nu)} \tag{11}$$

where σ_f is the flexural strength, ν is the Poisson ratio, E is the elastic modulus, and γ_{WOF} is the surface effective energy.

The unified theory (UT) of thermal shock fracture initiation and crack propagation in brittle materials [10,11] includes the parameters mentioned before, and defines a new parameter, the thermal stress crack stability parameter (R_{ST}). The R_{ST} parameter depends on the fracture surface energy (γ_{WOF}), the elastic modulus (E) and the linear thermal expansion coefficient (α). Once a crack has been initiated, thermal shock failure is controlled by the nature of the crack propagation through the material. This parameter can be used to predict the behavior of materials with sufficiently long cracks under severe thermal stresses. Some authors also state that the TSR can be correlated with the length of Lc, because it is proportional to R''''.

$$R_{ST} = \left[\frac{\gamma_{WOF}}{\alpha^2 E}\right]^{1/2} \tag{12}$$

According to Hasselman the first model is applicable to brittle materials where the crack initiation is determinant in the behavior. And the second approximation is valid where the initiation of the cracks is inevitable.

For the conditions used in this work it is reasonable to assume that the influence of the Biot ($h = \infty$) can be neglected to calculate R in the first model. Since composites studied can be taken as family of materials, the thermal conductivity (k) and surface energy are expected to be similar. Then the analysis can be reduced using Eqs. (8), (10) and (12) (R, R''' and R_{ST}).

4. Results and discussion

4.1. Materials characterization

The refractories (MRE S.A. Argentina; www.mre.com.ar) were fabricated by vibrocasting process and fired at 1450 °C. The refractory materials studied were called as: AZ, AM and Am. In Fig. 1 the diffraction patterns of the materials are shown. One of the materials (AZ) contains Zircon in its composition; little peaks of m-ZrO_2 were also detected indicating that a partial decomposition of Zircon occurs during calcinations of the refractory material. AM refractory has Mullite as a main principal phase. In Am the principal phase is Alumina accompanied by Mullite. The low background in all the

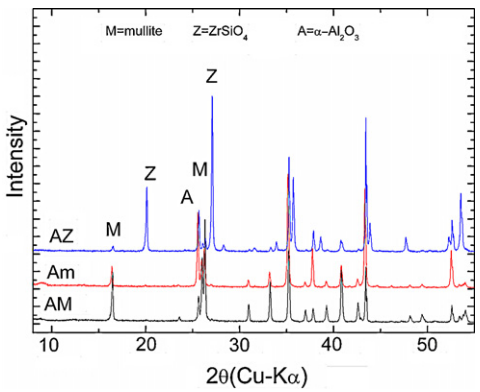

Fig. 1. DRX diffractograms of the studied materials.

Table 1
Properties and composition of the studied materials.

Material	Am	AM	AZ
Apparent density (g/cm^3)	2.7	2.6	3.2
Open porosity (%)	20	18	18
Principal crystalline phases	Alumina–Mullite	Mullite–Alumina	Alumina–Mullite–Zircon
Al_2O_3 (%)	90	80	69
SiO_2 (%)	9	18	9
ZrO_2 (%)	–	–	20
Fe_2O_3 (%)	0.3	0.3	0.3
$Na_2O + K_2O$ (%)	0.3	0.3	0.4
Matrix chemical composition (EDAX)			
Al_2O_3 (wt.%)	71	72	61
SiO_2 (wt.%)	29	28	15
ZrO_2 (wt.%)	0	0	24

samples indicates that the glassy phase present is not important. Their main physicochemical properties are shown in Table 1.

Open porosity of the materials using the Archimedes method is 18–20%. Pore size distributions (Hg intrusion) are shown in Fig. 2. Accumulative pore size curves are very similar for all three materials. Great pores are scarcely present and the average pore size is between 50 and 80 μm. No significant differences in pore size appeared.

Pores size and its contribution to total porosity may be a variable to consider for TSR. In this case porosity is not a parameter that can introduce differences on TSR materials behavior.

Thermal expansion coefficients (at 1000 °C) were very similar: Am: 7.0×10^{-6} °C, AM: 6.0×10^{-6} °C and AZ: 5.5×10^{-6} °C.

4.2. Microstructure

Micrographs from the polish materials (Am, AM and AZ) are shown in Figs. 3–5, respectively.

The microstructural analysis shows that:

- AZ material has a Zircon–Alumina–Mullite matrix, and tabular Alumina grains from fines to 4 mesh size.
- AM is made up by equal contents of Mullite grains (chamotte: it seems to be Mulcoa grains) and tabular Alumina in a wide range size (from 4 mesh to fines).
- Am presenting grains of tabular Alumina and grains of near 14 mesh size of a Mullite rich chamotte, in a fine Mullite–Alumina matrix.

Matrix chemical compositions of the three materials are shown in Table 1, showing that Am and AM have similar oxide contents while AZ matrix is of Alumina and Zircon without Mullite.

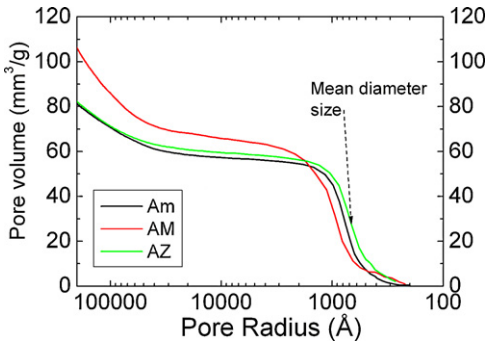

Fig. 2. Pore size distribution of the refractory materials studied.

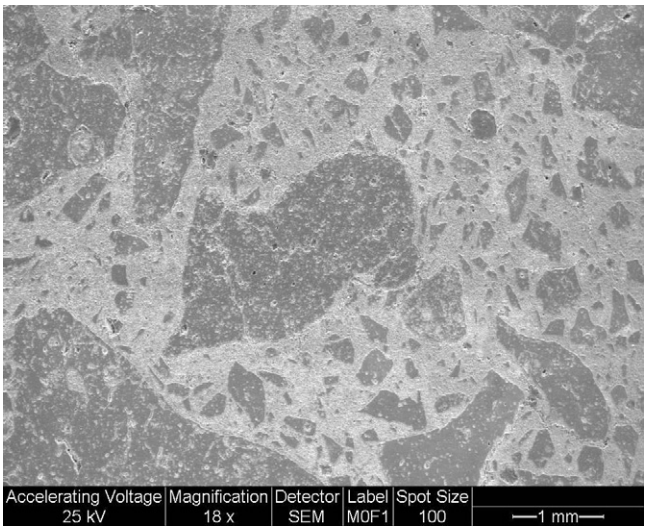

Fig. 3. SEM micrograph of the Am material (20×).

4.3. Mechanical and fracture properties

In Table 2 mechanical and fractures properties are shown. The flexural strength (σ_f) of the three materials is not high. AM presents the higher σ_f and E values, together with the higher toughness and lower work of fracture. Fracture initiation energy is similar for all materials. In Fig. 3 representative load–displacement curves

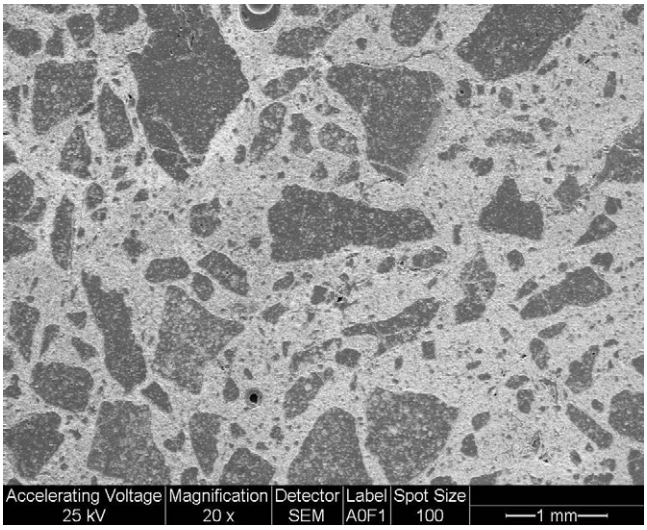

Fig. 4. SEM micrograph of the AM material (20×).

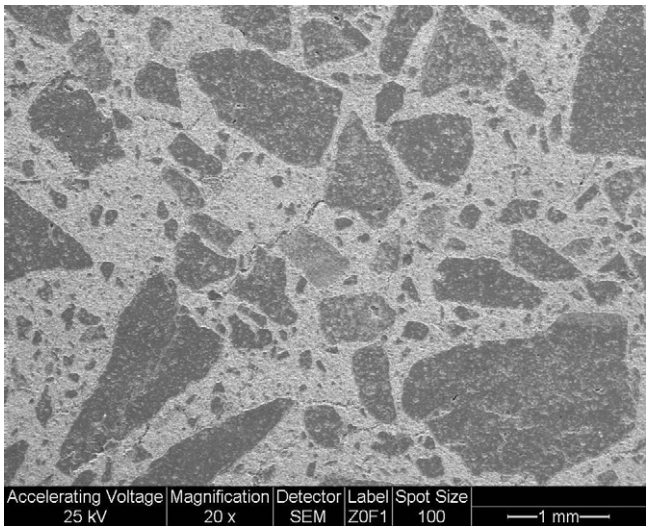

Fig. 5. SEM micrograph of the AZ material (20×).

for the notched bars are shown. For the three materials a stable fracture mechanism occurs. AM material has the higher strength value (σ_f) and showed a tendency to a brittle (semi-stable) fracture mechanism. The γ_{WOF} is more representative of the energy required to propagate a crack over a large area, rather than that to initiate fracture, e.g., the spalling resistance after initiation of crack propagation. The γ_{WOF} is usually interpreted as the work done in propagating a crack to break a notched specimen, divided by twice the fracture surface areas. The area under the load–displacement measured is strongly dependent on the notch depth, which can affect the fracture behavior. When a sufficiently deep notch is present, the total stored energy becomes small compared with the surface energy required to break the specimen. The γ_{NBT} is a measure of resistance to the initiation of crack propagation rather than the energy required to propagate a crack completely through a specimen. Various factors contribute to fracture surface energy. For materials undergoing a glass-like fracture, crack initiation is more difficult than crack propagation ($\gamma_{NBT} > \gamma_{WOF}$) because of the multiplicity of surface crack sources. A material containing many small cracks may therefore be more resistant to catastrophic failure than a material containing few small cracks. In contrast, materials containing many volume crack sources, such as refractories, show a greater resistance to crack propagation than to crack initiation ($\gamma_{NBT} < \gamma_{WOF}$). For our samples γ_{NBT} is clearly lower than γ_{WOF} (10 times). Toughness (K_{IC}) and E are clearly high in AM material.

Fig. 6 shows examples of the load–displacement (with 0.1 mm/min displacement rate) curves used for the γ_{WOF} measurements for the studied materials: none of them could be defined as fragile materials, the three materials retain some important cohesive energy once they overcome the maximum load. For Am and AZ a stable fracture behavior is observed, but for AM a semi-stable fracture was identified.

Table 2
Mechanical and fracture properties of the studied materials.

Material	Am	AM	AZ
σ_{f0} (MOR) (MPa)	12.8	17.2	13.0
E_0 (GPa)	30.0	59.0	30.4
K_{IC} (MPa m$^{1/2}$)	0.61	0.88	0.62
γ_{WOF} (J/m^2)	77	59	66
γ_{NBT} (J/m^2)	6.4	6.6	6.4

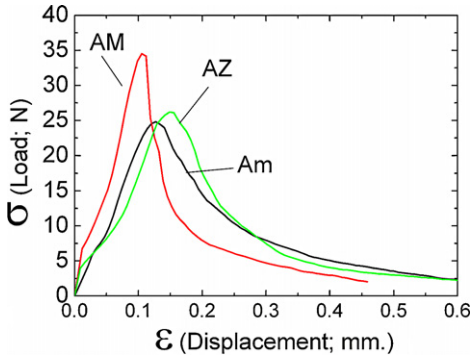

Fig. 6. Examples of the load–displacement graphs obtained from the bars.

5. Thermal shock results

The microstructural observation (SEM) of the samples submitted to sudden temperature gradients revealed a microstructural degradation that was also detected through the decrease in the mechanicals properties (dynamic elastic modulus and mechanical strength).

5.1. Microstructural observation of the thermal shock damage

SEM micrographs of the quenched and polished samples are shown in Figs. 7–9. Images were taken from materials submitted to quenching treatments of 1000 °C. In all the materials long cracks (several millimeters) were detected evidencing an important microstructural degradation. In the Zirconia free refractories (Am and AM) three types of cracks were identified:

- Cracks within the matrix.
- Cracks in the chamotte–matrix interface (grain boundary).
- Cracks in the Alumina grains.

In Figs. 7 and 8, examples of the cracks, were labeled A–C, respectively. While in the AZ material the third cracks were not detected (Fig. 9), this fact shows that being submitted to the same thermal treatment the microstructural degradations presented is lower.

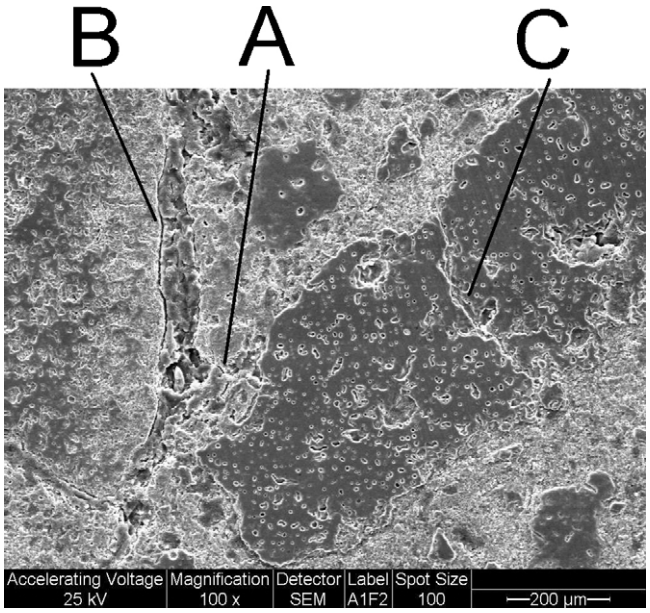

Fig. 7. The (×60) should be replaced by a (×100).

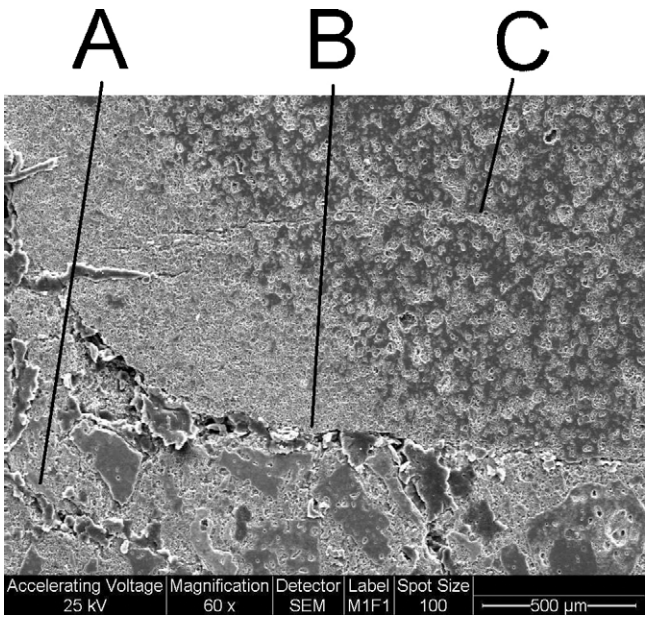

Fig. 8. The (×100) should be replaced by a (×60).

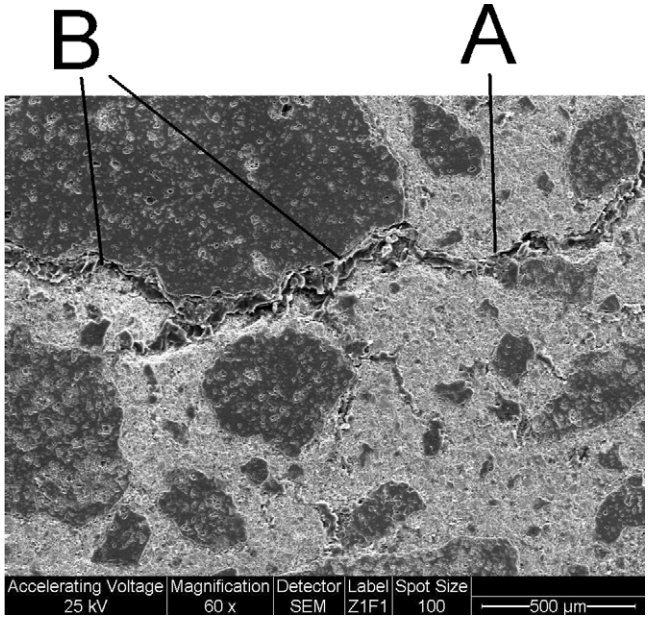

Fig. 9. The (×100) should be replaced by a (×60).

Although this differentiation could be done, this was only rough and a more global and systematic analysis is concluding.

5.2. Evaluation of the thermal shock resistance (TSR)

In the present work the effect of the quenching treatment on the elastic modulus and flexural strength was measured.

Firstly the TSR was evaluated by measuring the decrease in E/E_0 ratio where E_0 and E are the original elastic modulus and that after one quenching, respectively. Fig. 10 shows the evolution of E/E_0 ratio, with ΔT. The E/E_0 remained unchanged up to ΔT near 300 °C for all materials, whereas a reduction of E/E_0 was caused by more severe shocks. This indicates that the degree of damage was not significant up to $\Delta T \approx 400$ °C while it grows when the applied ΔT increased up to 1000 °C. Thus, the ΔTc of the materials was near

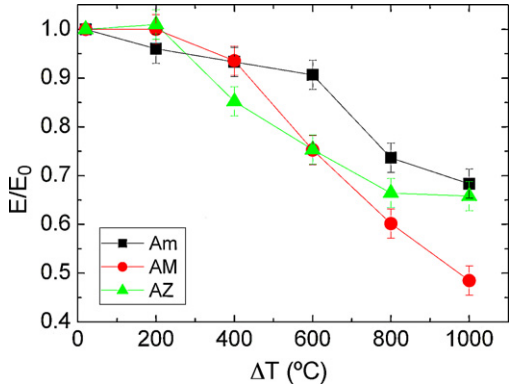

Fig. 10. Effect of quenching temperature differences (ΔT) on E/E_0 ratio (TSR).

to 400 °C. At higher ΔT (800 and 1000 °C) a clear decay in E/E_0 is observed for AM material.

Secondly, Fig. 11 shows the evolution of the σ_f/σ_{f0} (MOR ratio) after the quenching treatment. The decay of strength is more pronounced than E. A clear difference of the behavior is showed up to a $\Delta T = 600$ °C. Strength and E decay in a similar form for the studied materials, indicating a high TSR for AZ and Am materials when $\Delta T = 800$ and 1000 °C are considered.

Figs. 10 and 11 show a continuous decrease with the ΔT of both mechanical properties, suggesting a quasi-static crack growth [21], in concordance with the mechanical behavior shown in Fig. 6. For these materials both flexural strength and the elastic modulus are inversely proportional to the number (density) and size (size distributions) of the developed cracks in the microstructure of the material [25].

For refractory castables a logarithmic relation between these two ratios was shown in a previous work [20]

$$\left(\frac{E}{E_0}\right) = \left(\frac{\sigma_f}{\sigma_{f0}}\right)^{2/n} \tag{13}$$

After logarithms this can be rewritten as follows. The value for n found for refractory castables in Ref. [20] was 0.488.

$$\ln\left(\frac{E}{E_0}\right) = \frac{2}{n}\ln\left(\frac{\sigma_f}{\sigma_{f0}}\right) = B\ln\left(\frac{\sigma_f}{\sigma_{f0}}\right) \tag{14}$$

Fig. 12 plots this logarithmic graph for the three materials studied (superposed) showing also a linear behavior. The slope value B derived from the linear fit carried out for the ratios evaluated is equal to $2/n$ (Eq. (14)). The value of n found for these materials is 2.6. This difference demonstrates that the strength degradation of these refractory materials can be predicted from dynamic measurements but that the value of n is not a universal constant. As the dynamic measurements are non-destructive this will bring an important operative saving in the materials mechanical and thermomechanical characterization.

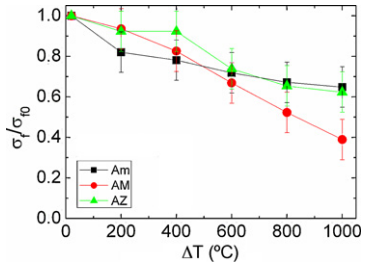

Fig. 11. Effect of quenching temperature differences (ΔT) on σ_f/σ_{f0} ratio (TSR).

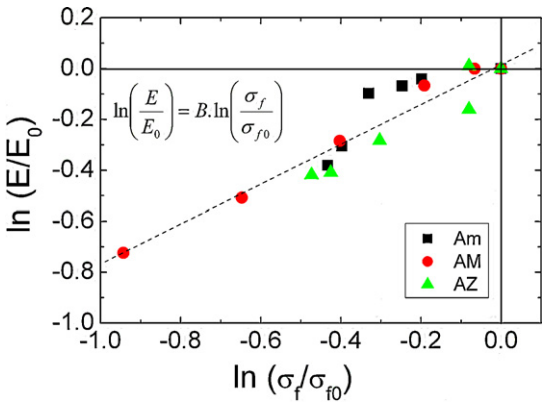

Fig. 12. Correlation of the decrease of σ_f and E.

5.3. Evaluation of the thermal fatigue resistance (TFR)

The effect of the number of quenching cycles on the E/E_0 ratio is graphed in Fig. 13 for $\Delta T = 500\,^{\circ}C$ and $\Delta T = 1000\,^{\circ}C$ cyclic quenching tests, respectively.

There was a rapid E/E_0 drop after few cycles, and then a gradual reduction up to achieving a saturation value (named E_f/E_0) as the number of cycles increased. The materials reach a situation where the thermal treatment does not introduce further damage in the microstructure as is reflected by the E/E_0 values. This is a typical behavior previously reported in the literature [19–23,25–28].

In the test carried out with $\Delta T = 500\,^{\circ}C$ no important difference between the studied refractories is observed. TFR test with $\Delta T = 1000\,^{\circ}C$ differences between the refractories are observed.

Materials response to this test is more precise than the one obtained in the TSR tests shown in Section 5.2. The AM material was the most damaged, retaining only the 25% of the original elastic modulus after five thermal cycles. While Am and AZ material showed a better performance retaining ≈50% of the original E value. Moreover the material containing ZrO_2 in the binding matrix (AZ) presented the best TFR, evaluated by the evolution of the elastic constant of the materials by the non-destructive impulse excitation technique.

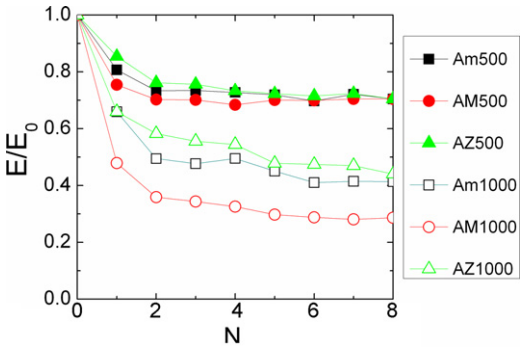

Fig. 13. Effect of number of thermal cycling in the E/E_0 ratio (TFR) using a ΔT of 500 and 1000 °C.

The saturation value of the elastic modulus retention (E_f/E_0), with $\Delta T = 1000\,^{\circ}C$, showed to be a satisfactory experimental parameter to evaluate the TFR brittle ceramic materials. Values of the saturation values (σ_{f8} and E_8) and saturation ratios (σ_{f8}/σ_{f0} and E_8/E_0) are included in Table 3.

5.4. Theoretical and experimental thermal shock resistance parameters

In Table 3, calculated TSR parameters using mechanical and fracture values are also listed. In the same table experimental parameters are included: σ_f/σ_{f0} and E/E_0 at a $\Delta T = 1000\,^{\circ}C$. These experimental parameters indicate that Am and AZ materials have a similar TSR behavior and AM has a clearly lower TSR. This fact is in concordance with the one observed when these refractories are used by customers in the glass feeders.

The parameters considering crack initiation (R) are very similar for all materials but quite different from those observed experimentally (ΔTc). This fact can be explained if we consider that microstructure of refractories have initially defects and microcracks. The R''' parameters are the same for all materials, so, this parameter do not reflect experimental data.

In terms of the R'''' thermal shock parameter, the $\gamma_{WOF}/\gamma_{NBT}$ ratio is a clear manifestation of the increase in crack resistance with crack extension. The larger the $\gamma_{WOF}/\gamma_{NBT}$ ratio, the smaller the strength degradation normally associated with thermal quenching of a specimen from above a sufficient temperature enough to initiate strength degradation.

A large $\gamma_{WOF}/\gamma_{NBT}$ ratio is in this theory a fundamental requirement for a good thermal shock damage resistance. For refractory materials the $\gamma_{WOF}/\gamma_{NBT}$ ratio in many cases is found to be a reliable indicator, as well as the R'''' thermal shock parameter, to determine crack propagation resistance after thermal shock. The R'''' values for our materials are relatively large compared to those of dense ceramic materials. Considering $\gamma_{WOF}/\gamma_{NBT}$ values: Am has the highest TSR, followed by AZ, while AM has the lowest TSR; however, the difference between these values does not clearly reflect the experimental data (σ_f/σ_{f0} and E/E_0).

The unified theory of thermal shock fracture initiation and crack propagation defines a new parameter, the thermal stress crack stability parameter (R_{ST}). The R_{ST} parameter depends on the fracture surface energy (γ_{NBT}), the elastic modulus (E) and the linear thermal expansion coefficient (α). Once a crack has been initiated, thermal shock failure is controlled by the nature of the crack propagation

Table 3
Thermal shock resistance parameters (experimental and theoretical).

Material		Am	AM	AZ
Experimental thermal shock resistance parameters	σ_f/σ_{f0} ($\Delta T = 1000\,^{\circ}C$)	0.65	0.39	0.62
	E/E_0 ($\Delta T = 1000\,^{\circ}C$)	0.68	0.49	0.66
Experimental thermal fatigue resistance parameters	σ_{f8} (MPa; $\Delta T = 1000\,^{\circ}C$)	8.2	6.5	9.2
	σ_{f8}/σ_{f0} ($\Delta T = 1000\,^{\circ}C$)	0.64	0.38	0.71
	E_8 (GPa; $\Delta T = 1000\,^{\circ}C$)	13.2	17.0	14.7
	E_8/E_0 ($\Delta T = 1000\,^{\circ}C$)	0.44	0.29	0.48
Theoretical thermal shock resistance parameters	R (ΔT_C)	63	41	56
	R''' (MPa^{-1})	183	199	180
	Lc (R'''', cm)	1.4	1.1	1.2
	R_{ST} (mK^2)	10.1	6.3	9.3
	$\gamma_{WOF}/\gamma_{NBT}$	12.0	8.9	10.3

through the material. The R_{ST} parameter defines the propagation of inherent, pre-existing cracks in a refractory and for our materials the R_{ST} parameter reflected the TSR damage observed in the experimental data (σ_f/σ_{f0} and E/E_0).

The best TSR resistance of AZ and Am is due to the microcracks sizes and their distribution in the microstructure of the materials. These materials are also the most elastic (low E) and have a lower strength compared to that of AM.

With respect to TFR the values obtained for the saturation relations of σ_f and E (N = 8 and ΔT = 1000 °C) are in accordance with the TSR experimental parameters.

6. Conclusions

Three refractories employed in the glass industry where analyzed to observe if their TSR behavior in service may be correlated with experimental TSR and TFR tests together with the theoretical TSR parameters calculated from mechanical and fracture properties.

The impulse excitation technique was a useful method to evaluate the elastic modulus and therefore, was a satisfactory method to evaluate the microstructural damage consequence of the thermal shock in the refractory materials.

The value of E/E_0 or σ_f/σ_{f0} measured after TSR using a thermal difference (ΔT) of 1000 °C was a suitable parameter to compare and evaluate the TSR behavior of refractory materials. Considering that the E measure using the dynamic excitation method is an easy and non-destructive technique, it is preferred to the flexural strength test to evaluate TSR.

Furthermore, the saturation value of the elastic modulus retention (E_f/E_0), with ΔT = 1000 °C, showed to be a satisfactory experimental parameter to evaluate the TFR brittle ceramic materials.

The thermoelastic theory does not reflect the TSR behavior, as is commonly observed in refractory materials.

The values of the characteristic lengths (Lc) indicate that the linear elastic fracture theory may be applied to materials of this size.

The R'''' values calculated from surface energies for our materials are relatively large compared to those of dense ceramic materials. Considering $\gamma_{WOF}/\gamma_{NBT}$ values: Am has the highest TSR, followed by AZ, being AM the one with the lowest TSR. However, the difference between these values does not clearly reflect the experimental data (σ_f/σ_{f0} and E/E_0).

The R_{ST} parameter reflected the TSR damage observed in the experimental data (σ_f/σ_{f0} and E_f/E_0).

The evolution of the dynamic elastic modulus and flexural strength (σ_f) measurements has shown to be suitable for the evaluation of TSR and TFR. Both behaviors are correlated for these materials.

The evolution of the refractory TSR can be made measuring the elastic modules relation using a quenching temperature difference of 1000 °C in an easy and inexpensive way.

References

[1] D.E. Parkinson, Glass Technol. 29 (1988) 73–176.
[2] E.A. Thomas, T. Weichert, Proc. UNITECR (1989) 730–760.
[3] G.F. Comstock, J. Am. Ceram. Soc. 16 (1) (1933) 12–35.
[4] T. Mori, Y. Yamada, H. Yamamura, H. Kobayashi, T. Mitamura, J. Ceram. Soc. Jpn. 100 (3) (1992) 250–258.
[5] W.D. Kingery, J. Am. Ceram. Soc. 38 (1) (1955) 3–15.
[6] F.E. Norton, J. Am. Ceram. Soc 8 (1) (1925) 29–39.
[7] C.E. Semler, R&A News 13 (1) (2008) 18–22.
[8] C.E. Semler, R&A News 13 (2) (2008) 18–24.
[9] ASTM Standard C-1525-04 Standard Test Method for Determination of Thermal Shock Resistance for Advanced Ceramics by Water Quenching, American Society for Testing and Materials, ASTM International, West Conshohoken, 2004.
[10] ASTM C1171-05 Standard Test Method for Quantitatively Measuring the Effect of Thermal Shock and Thermal Cycling on Refractories, 2005.
[11] D.H.P. Hasselman, J. Am. Ceram. Soc. 52 (11) (1969) 600–604.
[12] D.H.P. Hasselman, Am. Ceram. Soc. Bull. 49 (12) (1970) 1033–1037.
[13] D.H.P. Hasselman, Mater. Sci. Eng. 71 (C) (1985) 251–264.
[14] C. Aksel, Mater. Lett. 57 (2002) 992–997.
[15] ASTM Standard C-1419-99a Test Method for "Sonic Velocity in Refractory Materials at Room Temperature and Its Use in Obtaining an Approximate Young's Modulus", vol. 151, 2001, 637 pp.
[16] M. Radovic, E. Lara-Curzio, L. Riester, Mater. Sci. Eng. A 368 (1) (2004) 56–70.
[17] J. Kübler, Ceram. Eng. Sci. Proc. 18 (4) (1997) 155–162.
[18] V. Pandolfelli, V. Salvini, Proc. UNITECR (1993) 282–291.
[19] H. Harmuth, E. Tsechegg, Veitsch-Radex-Rundschau 1–2 (1994) 465–542.
[20] S.K. Niyogi, A.C. Das, Interceram 43 (6) (1994) 453–457.
[21] W. Lee, E. Case, Mater. Sci. Eng. A 154 (1992) 1–9.
[22] V.R. Vedula, D.J. Green, J.R. Hellmann, J. Eur. Ceram. Soc. 18 (1998) 2073–2080.
[23] T. Tonnesen, R. Telle, Proc. UNITECR (2009) C-197.
[24] A.H.A. Pereira, A.E.M. Paiva, B. Schickle, T. Tonnesen, B. Musolino, J.A. Rodrigues, Proc. UNITECR (2009) C-111.
[25] R.C. Stiffler, D.P.H. Hasselman, J. Am. Ceram. Soc. 66 (3) (1983) C52–C53.
[26] N.M. Rendtorff, L.B. Garrido, E.F. Aglietti, Ceram. Int. 34 (8) (2008) 2017–2024.
[27] N.M. Rendtorff, L.B. Garrido, E.F. Aglietti, Mater. Sci. Eng. A 498 (1–2) (2008) 208–215.
[28] N.M. Rendtorff, L.B. Garrido, E.F. Aglietti, Ceram. Int. 35 (2) (2009) 779–786.